Effective Field Theories and Lattice QCD for the X Y Z frontier

Nora Brambilla[a,b,c,*]

[a] *Physik Department, Technische Universität München,*
James-Franck-Strasse 1, 85748 Garching, Germany

[b] *Institute for Advanced Study, Technische Universität München,*
Lichtenbergstrasse 2 a, 85748 Garching, Germany

[c] *Munich Data Science Institute, Technische Universität München,*
Walther-von-Dyck-Strasse 10, 85748 Garching, Germany

E-mail: nora.brambilla@ph.tum.de

Exotic states have been predicted before and after the advent of QCD. In the last decades they have been observed at accelerator experiments in the sector with two heavy quarks, at or above the quarkonium strong decay threshold and called X Y Z states. These states offer a unique possibility for investigating the dynamical properties of strongly correlated systems in QCD. I will show how an alliance of nonrelativistic effective field theories and lattice can allow us to address these states in QCD. In particular I will explain what are the opportunities and challenges of lattice QCD in this respect and which new tools should be developed.

The 38th International Symposium on Lattice Field Theory, LATTICE2021 26th-30th July, 2021
Zoom/Gather@Massachusetts Institute of Technology

*Speaker

1. Introduction

Exotic states, i.e. states with a composition different from a quark-antiquark or three quarks in a color singlet, have been predicted before and after the inception of QCD. In the last decades a large number of states, either with a manifest different composition (with isospin and electric charge different from zero) or with other exotic characteristics have been observed in the sector with two heavy quarks $Q\bar{Q}$, at or above the quarkonium strong decay threshold at the B-Factories, tau-charm and LHC and Tevatron collider experiments [1–4]. These states have been termed X, Y, Z in the discovery publications, without any special criterion, apart from Y being used for exotics with vector quantum numbers, i.e., $J^{PC} = 1^{--}$ (where J is the spin, P is the parity and C is the charge-conjugation quantum number). Meanwhile, the Particle Data Group (PDG) has proposed a new naming scheme [5], that extends the scheme used for ordinary quarkonia, in which the new names carry information on the J^{PC} quantum numbers, see [1] for more details.

Some of these exotics have quantum numbers that cannot be obtained with ordinary hadrons. In this case, the identification of these states as exotic is straightforward. In the other cases, the distinction requires a careful analysis of experimental observations and theoretical predictions. Of course all hadrons should be color singlets but allowing combinations beyond the $Q\bar{Q}$ and QQQ in the two heavy quarks sector calls for tetraquarks like $Q\bar{Q}q\bar{q}$, $QQ\bar{q}\bar{q}$, pentaquarks like $Q\bar{Q}qqq$, hybrids $Q\bar{Q}g$ and so on [7] . We have observed these exotics up to now only in the sector with two heavy quarks likely due to the fact that the presence of the two heavy quarks stabilizes them. *Some of the discovered states have an unprecedently and surprinsingly small width even if they are at or above the strong decay threshold. XYZ states offer us unique possibilities for the investigation of the dynamical properties of strongly correlated systems in QCD: we have by now measured their signatures in the spectrum and we should develop the tools to gain a solid interpretation from the underlying field theory, QCD. This is a very significant problem with trade off to other fields featuring strong correlations and a pretty interesting connections to heavy ion physics, as propagation of these states in medium may help us to scrutinize their properties.*

Since the new quarkonium revolution i.e. the discovery of the first exotic state, the $X(3872)$ at BELLE in 2003 [6], a wealth of theoretical papers appeared to supply interpretation and understanding of the characteristics of the exotics. Many models are based on the choice of some dominant degrees of freedom and an assumption on the related interaction hamiltonian. An effective field theory molecular description of some of these states particularly close to threshold was also put forward, see e.g. [8–11]. A priori the simplest system consisting of only two quarks and two antiquarks (generically called tetraquarks) is already a very complicated object and it is unclear whether or not any kind of clustering occurs in it. However, to simplify the problem it is common to focus on certain substructures and investigate their implications: in hadroquarkonia the heavy quark and antiquark form a compact core surrounded by a light-quark cloud; in compact tetraquarks the relevant degrees of freedom are compact diquarks and antidiquarks; in the molecular picture two color singlet mesons are interacting at some typical distance. Discussions about exotics therefore often concentrate on the 'pictures' of the states, like for example the tetraquark interpretation against the molecular one (of which both several different realizations exist). However, as a matter of fact all the light degrees of freedom (light quarks, glue, in different configurations) should be there in QCD close or above the strong decay threshold: it is a result of the strong dynamics which one sets

in and in which configuration dominates in a given regime. Even in an ordinary quarkonium or in a heavy baryon, which has a dominant $Q\bar{Q}$ or QQQ configuration, subleading contributions of the quantum field theoretical Fock space may contribute, with have additional quark-antiquark pairs and active gluons. *Addressed like that, the problem turns out to be extremely challenging. I will show how the presence of two heavy quarks gives us a way to simplify the problem and to address it using nonrelativistic effective field theories (NR EFTs) and lattice. The existence of a large scale, the scale of the mass of the heavy quark m, allows us to take advantage of scale factorization and to use lattice QCD to evaluate purely glue dependent correlators at the low energy scale. Such correlators are not depending on flavor and are universal, i.e. the can be evaluated once and used for prediction on a large number of states. I will argue that this method is complementary and often preferable with respect to an ab initio lattice evaluation of the properties of each single state.* To pursue this aim, i.e. to perform lattice evaluation directly on factorized low energy objects in the framework of EFTs, we have founded a dedicated lattice collaboration called TUMQCD [14].

The paper is organized in the following way: in section two I summarize how the combination of NREFTs and lattice has allowed us to address quarkonium properties in vacuum and in medium in QCD. In the following sections I put forward a similar framework for exotica. In particular in section three I introduce the so called BOEFT (Born Oppenheimer Effective Field Theory) to describe hybrids and I report the predictions of the theory and how progress depends on more precise and/or new lattice evaluations of low energy correlators, even quenched. In Section four I extend this description to states with light quarks, which would give a theory of the tetraquarks and molecular pictures. In also examine how heavy ion collisions can help us supplying complementary information and what is the role of the EFT and lattice in this. A list of lattice calculations that would be needed to gain progress is given in each section and in the outlook. In this latter I also discuss tools, methods and open challenges to get these low energy correlators from the lattice.

2. NREFTs and Lattice for Quarkonium

The study of quarkonium in the last few decades has witnessed two major developments: the establishment of NREFTs and progress in lattice QCD calculations of excited states and resonances, with calculations at light-quark masses. Both allow for precise and systematically improvable computations that are (to a large extent) model-independent. It is precisely this advancement in the understanding of quarkonium and quarkonium-like systems inside QCD that makes quarkonium exotics particularly valuable. *In fact, today that we are confronted with a huge amount of high-quality data, which have provided for the first time uncontroversial evidence for the existence of exotic hadrons, by using modern theoretical tools that allow us to explore in a controlled way these new forms of matter we can get a unique insight into the low-energy dynamics of QCD.*

2.1 Physical scales of quarkonium

Heavy quarkonia are systems composed by two heavy quarks (charm, bottom), with mass m larger than the "QCD confinement scale" Λ_{QCD}, so that $\alpha_{\text{s}}(m) \ll 1$ holds. From the quarkonia spectra it is evident that the difference in energy levels is much smaller than the quark mass and therefore quarkonia are nonrelativistic systems. As such they are multiscale systems. Being nonrelativistic, quarkonia are characterized by a small parameter, the heavy-quark relative velocity

$v = |\vec{v}|$ in the rest frame of the meson, where $v^2 \sim 0.1$ for the $b\bar{b}$, $v^2 \sim 0.3$ for $c\bar{c}$ systems. This parameter induces a hierarchy of dynamically generated energy scales: starting from the mass m of the heavy quark (hard scale), there is the typical relative momentum $p \sim mv$, corresponding to the inverse Bohr radius $r \sim 1/(mv)$ (soft scale), and a typical binding energy $E \sim mv^2$ (ultrasoft (US) scale). The description of the heavy $Q\bar{Q}$ systems depends finally on the relation of Λ_{QCD} to the above mentioned scales. Clearly, for energy scales close to Λ_{QCD} there is no longer any perturbative description and one has to rely on nonperturbative methods. Regardless of this, the nonrelativistic hierarchy $m \gg mv \gg mv^2$ persists also below the Λ_{QCD} threshold, as long as v is small. While the hard scale m is always assumed to be larger than Λ_{QCD}, different situations may arise for the other two scales.

The hierarchy of nonrelativistic scales makes the difference between heavy quarkonia and heavy-light mesons, which are characterized by just two scales: m and Λ_{QCD}. This renders the theoretical description of quarkonium much more complicated. All these scales get entangled in a typical amplitude involving a quarkonium observable. Moreover the nonrelativistic bound state problem is "nonperturbative", even at small α_s, i.e. infinite series of diagram needs to be resummed, differently from an on shell scattering calculation. Quarkonium annihilation and production take place at the scale m, quarkonium binding takes place at the scale mv, which is the typical momentum exchanged inside the bound state, while very low-energy (US) gluons and light quarks live long enough that a bound state has time to form and, therefore, are sensitive to the scale mv^2. US gluons are responsible for phenomena similar to the the Lamb shift in QED. To address this nonrelativistic multiscale system in quantum field theory is a real challenge. It is so even in QED with positronium and it is even more difficult here with the nonperturbative effects. Notice that even if you were interested in a lattice first principle simulations, still the existence of a set of widely separated scales will make the lattice calculation very challenging, The solution is to take advantage of the existence of the different energy scales to substitute QCD with simpler but equivalent NREFTs. A hierarchy of NREFTs may be constructed by systematically integrating out modes associated with high-energy scales not relevant for the quarkonium system. Such integration is made in a matching procedure that enforces the equivalence between QCD and the EFT at a given order of the expansion in v. The EFT Lagrangian is factorized in matching coefficients, encoding the high energy degrees of freedom and low energy operators. The relativistic invariance is realized via exact relations among the matching coefficients [15, 16]. The EFT displays a power counting in the small parameter v, therefore we are able to attach a definite power of v to the contribution of each EFT operators to the physical observables.

2.2 Physics at the scale m: NRQCD

Nonrelativistic QCD (NRQCD) [17, 18], follows from QCD integrating out the scale m. As a consequence, the effective Lagrangian is organized as an expansion in $1/m$ and $\alpha_s(m)$:

$$\mathcal{L}_{\text{NRQCD}} = \sum_n \frac{c_n(\alpha_s(m), \mu)}{m^n} \times O_n(\mu, mv, mv^2, ...), \tag{1}$$

where c_n are Wilson coefficients that contain the contributions from the scale m; they can be perturbatively calculated by matching the full QCD result to the EFT. The O_n are local operators of NRQCD; the matrix elements of these operators contain the physics of scales below m, in particular

of the scales mv and mv^2 and also of the nonperturbative scale Λ_{QCD}. Finally, the parameter μ is the NRQCD factorization scale. The low-energy operators O_n are constructed out of two or four heavy quark/antiquark fields plus gluons. The quarkonium states $|H\rangle$ in NRQCD is expanded in the number of partons

$$|H\rangle = |\bar{Q}Q\rangle + |\bar{Q}Qg\rangle + |\bar{Q}Q\bar{q}q\rangle + \cdots \tag{2}$$

where the states including one or more light parton are shown to be suppressed by powers of v. In the $|\bar{Q}Qg\rangle$ for example the quark-antiquark are in a color octet state. The NRQCD lagrangian has been extensively used on the lattice with great success by the HPQCD collaboration to calculate quarkonium spectra and decays[1]. On the other hand, NRQCD has been deeply impactful on the study of quarkonium production at the LHC putting forward a factorization formula for the inclusive cross section for the direct production of the quarkonium H at large momentum in the center of mass frame written as a sum of products of NRQCD matrix elements and short-distance coefficients:

$$\sigma[H] = \sum_n \sigma_n \langle \mathcal{K}_n^{\text{4fermions}} \rangle \tag{3}$$

where the σ_n are short-distance coefficients, and the matrix elements $\langle \mathcal{K}_n^{\text{4fermions}} \rangle$ are vacuum-expectation values of objects similar to the four-fermion operators in decays and containing both color singlet and color octet contributions. The matrix elements (LDMEs, long distance matrix elements) $\langle \mathcal{K}_n^{\text{4fermions}} \rangle$ contain all of the nonperturbative physics associated with the evolution of the $Q\bar{Q}$ pair into a quarkonium state. *Notice however that it has never been possible up to now to calculate these LDMEs on the lattice due to their cumbersome definition.*

2.3 Physics at the scale mv: pNRQCD

Quarkonium formation happens at the scale mv. The suitable EFT is potential non relativistic QCD, pNRQCD [19–21], which follows from NRQCD by integrating out the scale $mv \sim r^{-1}$. The soft scale mv may be either larger or smaller than the confinement scale Λ_{QCD} depending on the radius of the quarkonium system. When $mv \gg \Lambda_{\text{QCD}}$, we speak about weakly-coupled pNRQCD because the soft scale is perturbative and the matching from NRQCD to pNRQCD may be performed in perturbation theory. When $mv \sim \Lambda_{\text{QCD}}$, we speak about strongly-coupled pNRQCD because the soft scale is nonperturbative and the matching from NRQCD to pNRQCD is nonperturbative and cannot be calculated with an expansion in α_s. *The low energy nonperturbative factorized effects depend on the size of the physical system: when Λ_{QCD} is comparable or smaller than mv they are carried by correlators of chromoelectric or chromomagnetic fields nonocal or local in time, when Λ_{QCD} is of order mv they are carried by generalized static Wilson loops with insertion on chromoelectric and chromomagnetic fields.* The EFT allows us to make model independent predictions and we can use the power counting to attach an error to the theoretical prediction. *The nonperturbative phyiscs in pNRQCD is encoded in few low energy correlators that depend only on the glue and are gauge invariant: these are objects in principle ideal for lattice calculations.[2]*

---

[1]Notice that the NRQCD leading piece of the Lagrangian differently from the HQET one is not renormalizable, so that lattice calculation cannot go to the continuum limit but have to stay in the scaling window.

[2]We notice that leading piece of the pNRQCD lagrangian is renormalizable.

2.3.1 Weakly coupled pNRQCD

The lowest levels of quarkonium, like $J/\psi, \Upsilon(1S), \Upsilon(2S)\ldots$, may be described by weakly coupled pNRQCD, while the radii of the excited states are larger and presumably need to be described by strongly coupled pNRQCD. All this is valid for states away from strong-decay threshold, i.e. the threshold for a decay into two heavy-light hadrons. The effective Lagrangian is organized as an expansion in $1/m$ and $\alpha_s(m)$, inherited from NRQCD, and an expansion in r (multipole expansion) [21]:

$$L_{\text{pNRQCD}} = \int d^3R \int d^3r \sum_n \sum_k \frac{c_n(\alpha_s(m), \mu)}{m^n} V_{n,k}(r, \mu', \mu) \, r^k \times O_k(\mu', mv^2, \ldots), \quad (4)$$

where $\mathbf{R}$ is the center of mass position and O_k are the operators of pNRQCD. The matrix elements of these operators depend on the low-energy scale mv^2 and μ', where μ' is the pNRQCD factorization scale. The $V_{n,k}$ are the Wilson coefficients of pNRQCD that encode the contributions from the scale r and are nonanalytic in r. The c_n are the NRQCD matching coefficients as given in (1).

The degrees of freedom, which are relevant below the soft scale, and which appear in the operators O_k, are $Q\overline{Q}$ states (a color-singlet S and a color-octet $O = O_a T^a$ state, depending on $\mathbf{r}$ and $\mathbf{R}$) and (ultrasoft) gluon fields, which are expanded in r as well (multipole expanded and depending only on $\mathbf{R}$). pNRQCD makes apparent that the correct zero order problem is the Schrödinger equation. Looking at the equations of motion of pNRQCD, we may identify $V_{n,0} = V_n$ with the $1/m^n$ potentials that enter the Schrödinger equation and $V_{n,k\neq 0}$ with the couplings of the ultrasoft degrees of freedom, which provide corrections to the Schrödinger equation. Nonpotential interactions, associated with the propagation of low-energy degrees of freedom are, in general, present as well, and start to contribute at NLO in the multipole expansion. *They are typically related to nonperturbative effects and are carried by purely gluonic correlator local or nonlocal in time: they need to be calculated on the lattice.* pNRQCD enables precise and systematic higher order calculations on bound state allowing the extraction of precise determinations of standard model parameters like the quark masses and α_s from quarkonium.

2.4 Strongly coupled pNRQCD

When $mv \sim \Lambda_{\text{QCD}}$ the soft scale is nonperturbative, the matching cannot be performed in perturbation theory any more. Only singlet degrees of freedom exist and they include $Q\bar{Q}$ states, hybrids $Q\bar{Q}g$ states and glueballs. *Since the physics is nonperturbative we need to use* **lattice input** *to construct the EFT*. In particular we need the lattice evaluation of the gluonic static energies of $Q\bar{Q}$ pair: the have been calculated on the lattice since long [22–24] and recently updated in [25, 26] and they use generalized Wilson loops. The gluonic static energies, E_Γ in Fig. 2, are classified according to representations of the symmetry group $D_{\infty h}$, typical of molecules, and labeled by Λ_η^σ (see Fig. 1): Λ is the rotational quantum number $|\hat{\mathbf{r}} \cdot \mathbf{K}| = 0, 1, 2, \ldots$, with $\mathbf{K}$ the angular momentum of the gluons, that corresponds to $\Lambda = \Sigma, \Pi, \Delta, \ldots$; η is the CP eigenvalue ($+1 \equiv g$ (gerade) and $-1 \equiv u$ (ungerade)); σ is the eigenvalue of reflection with respect to a plane passing through the $Q\bar{Q}$ axis. The quantum number σ is relevant only for Σ states. In general there can be more than one state for each irreducible representation of $D_{\infty h}$: higher states are denoted by primes, e.g., Π_u, Π_u', Π_u'', $\ldots$ *This set of static energies will be fundamental to address the exotics.*
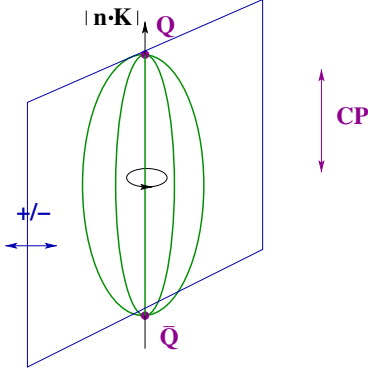
Figure 1: Quarkonium hybrid symmetries.
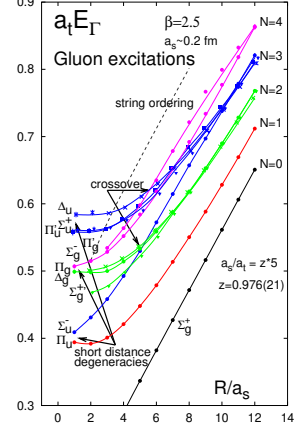
Figure 2: Hybrid static energies, E_Γ, in lattice units, from [23].

Since at this moment we are dealing with $Q\bar{Q}$ states below threshold we are interested merely in Σ_g^+ static energy (that in this case coincides with the static singlet $Q\bar{Q}$ potential) and in the information that such curve develops a gap of order Λ_{QCD} at a distance $r \sim \Lambda_{\text{QCD}}^{-1}$: therefore all the hybrid static energies can be integrated out as pNRQCD follows from integrating out all degrees of freedom with energy up to mv^2. The quarkonium singlet field $S = \bar{Q}Q$ is the only low-energy dynamical degree of freedom in the pNRQCD Lagrangian (up to US pions) which reads [19, 27, 28]:

$$L_{\text{pNRQCD}} = \int d^3R \int d^3r \, S^\dagger \left(i\partial_0 - \frac{\mathbf{p}^2}{2m} - V_S(r) \right) S \tag{5}$$

and lends support to potentials models in this regime, with the difference that the singlet potential $V_s(r) = V_0 + V_1/m + V_2/m^2$ is the QCD potential calculated in the matching [27, 28] and appear to have differences with respect to the phenomenological potential models. The potential at order $1/m^2$ contains a velocity dependent and a spin dependent part, with a spin orbit, spin-spin and spin tensor interaction. *Notice that spin effects are appearing only at order $1/m^2$ and are therefore suppressed in the spectrum and in the transitions: we will see that things are different for exotics. These potentials are nonperturbative quantities in the form of expectation values of generalized (with chromolectric and chromomagnetic insertions) gauge invariant Wilson-loop operators to be evaluated on the lattice. Actually it is the EFT that lends a clean definition and an interpretation of the static Wilson loops measured on the lattice as actual potentials in this regime, together with a prescription to use them to calculate observables. Some of these generalized Wilson loops have been calculated on the lattice (only quenched) [30–34] but some contributions at order $1/m^2$ are still to be calculated.* Using these potentials, all the masses for heavy quarkonia away from threshold can be obtained by the solution of the Schrödinger equation with such potentials. Lorentz invariance is still there in the form if exact relations among potentials and it has been observed on the lattice. Decays are described by calculating the imaginary parts of the potentials [35] where nonperturbative contributions enter in the form of gauge invariant time non local chromoelectric and

7

chromomagnetic correlators that have still to be calculated on the lattice. Summarizing, strongly coupled pNRQCD factorizes low energy nonperturbative contributions in terms of generalised gauge invariant Wilson loops opening the way to a systematic study of the confinement mechanism and systematic applications to quarkonium spectrum and decay.

2.4.1 Quarkonium production

NRQCD is the theory used to study quarkonium production, however one of the main problem is the proliferation of LDMEs, i.e. the nonperturbative matrix elements of singlet and octet four fermions operators: they are flavor dependent and increase in number when one seeks precision in the expansion in v. While those containing singlet operators can be reduced to the wave functions, the octet ones had to be extracted from the data, with contradictory results. The lower energy factorization obtained in pNRQCD may have a great impact also on quarkonium production: it has been shown that, for the case of inclusive quarkonium production in P wave, the octet LDMEs can be factorized in the product of the quarkonium wave function derivative in the origin and a chromoelectric correlator [36, 37]

$$\langle\Omega|O^{h_Q}(^1S_0^{[8]})\Omega\rangle = 3 \times \frac{3N_c}{2\pi}|R^{(0)\prime}(0)|^2\frac{1}{9N_cm^2}\mathcal{E},$$ (6)

where $\mathcal{E}$ is the dimensionless gluonic correlator

$$\mathcal{E} = \frac{3}{N_c}\int_0^\infty dt\, t\, \int_0^\infty dt'\, t'\, \langle|\Omega|\Phi_\ell^{\dagger ab}\Phi_0^{\dagger ad}(0;t)gE^{d,i}(t)gE^{e,i}(t')\Phi_0^{ec}(0;t')\Phi_\ell^{bc}|\Omega\rangle.$$ (7)

where Φ_ℓ is a Wilson line along the (arbitrary) direction ℓ (up to infinity) in the adjoint representation and $|\Omega\rangle$ is the QCD vacuum state. This is similar to what one gets in the decay factorization of the NRQCD matrix elements [35]

$$\langle h_Q|\psi^\dagger T^a\chi\chi^\dagger T^a\psi|h_Q\rangle = \frac{3N_c}{2\pi}|R^{(0)\prime}(0)|^2\frac{1}{9N_cm^2}\mathcal{E}_3,$$ (8)

where the correlator $\mathcal{E}_3$ is defined by

$$\mathcal{E}_3 = \frac{1}{2N_c}\int_0^\infty t^3\, dt\langle\Omega|gE^{a,i}(t)\Phi_0^{ab}(t,0)gE^{b,i}(0)|\Omega\rangle.$$ (9)

Hence the pNRQCD expressions have more predictive power than the corresponding NRQCD ones. In particular, correlators determined with charmonium data may be used to compute color octet matrix elements and hence observables in the bottomonium sector.

2.5 Quarkonium in medium

pNRQCD has been extended to the case of finite temperature T which allows to calculate in the weak coupling the finite T quarkonium interaction potential and the thermal effects to the energies and widths [38]. In the strong coupling the potential is obtained from a lattice calculation of the Wilson loop at finite T [39]. In particular combining pNRQCD and open quantum system [41], it has been possible to describe the nonequilibrium evolution of small quarkonia systems (bottomonium) inside the strongly coupled Quark Gluon Plasma in the hierarchy $m \gg 1/r \gg T, m_D \gg mv^2$

with an evolution equation for the singlet and octet density matrix of the Linblad type [42]. The interesting thing is that the properties of the strongly coupled QGP are carried just by two transport coefficients that are appropriate correlators of electric fields at finite T [41]:

$$\kappa = \frac{g^2}{6N_c}\text{Re} \int_{-\infty}^{\infty} ds \left\langle \text{T}E^{a,i}(s)\phi^{ab}(s,0)E^{a,i}(0)\right\rangle, \gamma = -\frac{g^2}{6N_c}\text{Im} \int_{\infty}^{\infty} ds \left\langle \text{T}E^{a,i}(s)\phi^{ab}(s,0)E^{a,i}(0)\right\rangle,$$
(10)

where $\langle \ldots \rangle$ is a shortcut to indicate the QCD average at finite T on the QCD vacuum $|\Omega\rangle$ (and T is time ordering.) The quantity κ is the heavy quark momentum diffusion coefficient. κ has been evaluated on the lattice [43] for a medium locally in equilibrium at a temperature T. In particular, it is important to obtain their T dependence in a large range of T as done in [29]. Using the EFT one can relate these transport coefficients to the thermal modification of the energy levels and to the thermal widths of quarkonium, which allows us to use unquenched lattice calculations [44, 45] to determine them [40].

This formalism can be extended to describe the evolution of exotic states inside the QGP created in heavy ion collisions.

## 2.6 Role of the Lattice and Input needed from Lattice

Summarizing, for what concerns quarkonium below threshold, lattice results have been key in order to formulate strongky coupled pNRQCD and lattice input is still needed, precisely, we need:

- Lattice calculation of chromoelectric and chromomagnetic correlators local in time and nonlocal in time: they contribute to quarkonia spectra and decay [19, 35].

- Lattice calculation of generalized static Wilson loops with insertions of chromoelectric and chromomagnetic fields: they contain the information on the nonperturbative singlet static potential and its relativistic corrections.

- Lattice calculation of the chromolelectric correlators appearing in production: they allow to calculate the LDMEs necessary to describe quarkonium production. They are somehow similar to what is done for TMDs and PDFs.

- Lattice calculation of the transports coefficients: finite T lattice calculations of such objects in a wide range of T will enable us to use the lattice to study nonequilibrium processes [29, 41, 42]. There is not a yet a direct evaluation of γ.

This will be instrumental to sharpen our control of quarkonium spectrum, decays, production and propagation in medium and **to prepare for the treatment of the exotics.**

3. Exotics at or above the strong decay threshold

In the most interesting region, close or above the strong decay threshold, where the X Y Z have been discovered, the situation is much more complicated: there is no mass gap between quarkonium and the creation of a heavy-light mesons couple, nor to gluon excitations, therefore many additional states built on the light quark quantum numbers may appear. The threshold region
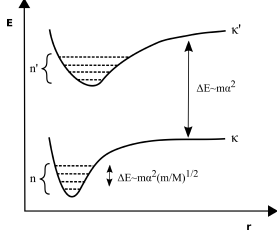
Figure 3: Electronic static energies in QED
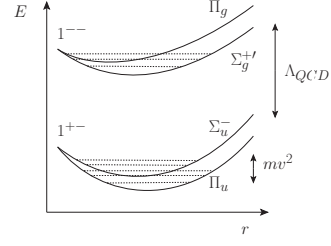
Figure 4: Gluonic (or Hybrid) static energies, E_Γ, in QCD.

remains troublesome also for the lattice, although several ab initio calculations of the exotic masses have been recently being pionereed. Still, m is a large scale and NRQCD is applicable. Then, if we want to introduce a description of the bound state similar to pNRQCD, making apparent that the zero order problem is the Schrödinger equation, we can still count on scale separation. Let us consider bound states of two nonrelativistic particles and some light d.o.f., e.g. molecules in QED or quarkonium hybrids ($Q\bar{Q}g$ states) or tetraquarks ($Q\bar{Q}q\bar{q}$ states) in QCD: electron/gluon fields/light quarks change adiabatically in the presence of heavy quarks/nuclei. The heavy quarks/nuclei interaction may be described at leading order in the nonrelativistic expansion by an effective potential V_κ between the static sources where κ labels different excitations of the light degrees of freedom. A plethora of states can be built on each on the potentials V_κ by solving the corresponding Schrödinger equation, see Figs. 3 and 4. This picture corresponds to the Born-Oppenheimer (BO) approximation. Starting from pNRQED/pNRQCD the BO approximation can be made rigorous and cast into a suitable EFT called Born-Oppenheimer EFT (BOEFT) [51–54, 58, 59] which exploits the hierarchy of scales $\Lambda_{\text{QCD}} \gg mv^2$ (the analogous in QED of the energy of the electrons being greater than the energy of nuclei or conversely the typical time of the electrons (fast degrees of freedom) being bigger than the typical time of the nuclei (slow degrees of freedom)). *BOEFT allows to address all exotics pictures (hybrids, tetraquarks, molecules and pentaquarks) in the same framework. Of course in QCD the scale Λ_{QCD} is nonperturbative and we need to use the lattice to calculate the appropriate gluonic static energies, see Fig. 2.*

3.1 Hybrids: Born Oppenheimer Effective Field Theory

In the following we consider the example of hybrids, i.e. states made by $Q\bar{Q}g$. We consider hybrids static energies that are labelled by the quantum numbers Λ_η^σ, see Sec. 2.4 and Fig. 2 and we restrict to considering the two lowest-lying static energies ones Π_u and Σ_u^-. Modes associated to higher potentials are separated from the Π_u and Σ_u^- potentials by an energy gap of order Λ_{QCD} and are integrated out with that scale. In the $r \to 0$ limit Π_u and Σ_u^- are degenerate and correspond to a gluonic operator with quantum numbers $\kappa \equiv K^{PC} = 1^{+-}$, $\mathbf{K}$ being the gluon angular momentum, because the group $D_{\infty h}$ becomes the more symmetric group O(3)×C [19, 21, 22]. We recall that λ is the quantum number $\lambda \equiv \mathbf{K} \cdot \hat{r}; |\lambda| = \Lambda$.

The hybrid static energies are defined by (Γ stays for Λ_η^σ)

$$E_\Gamma(r) = \lim_{T \to \infty} \frac{i}{T} \log\langle X_\Gamma, T/2 | X_\Gamma, -T/2\rangle; \quad |X_\Gamma\rangle = \chi(\mathbf{x}_2)\phi(\mathbf{x}_2, \mathbf{R})T^a P_\Gamma^a(\mathbf{R})\phi(\mathbf{R}, \mathbf{x}_1)\psi^\dagger(\mathbf{x}_1)|\Omega\rangle$$

$$(11)$$

where P_Γ^a is some gluonic operator that generates the right quantum numbers Γ. For our case we have $P_\Gamma^a = \hat{\mathbf{r}} \cdot \mathbf{B}^a, \hat{\mathbf{r}} \times \mathbf{B}^a$ respectively for the Σ_u^- and the Π_u, $\mathbf{B}^a$ being the chromomagnetic field. In the short-interquark-distance limit $r \to 0$, quarkonium hybrids reduce to gluelumps, which are color-singlet combinations of a local static octet color $Q\bar{Q}$ source coupled to a gluonic field [21, 51]. We define the gluelump operators, G_κ^{ia}, as the Hermitian color-octet operators that generate the eigenstates of the zero order NRQCD Hamiltonian H_0 in the presence of a local heavy-quark-antiquark octet source:

$$H_0 G_\kappa^{ia}(\mathbf{R}, t)|0\rangle = \Lambda_\kappa G_\kappa^{ia}(\mathbf{R}, t)|0\rangle\,, \tag{12}$$

where a is the color index and i the spin component (it labels the component of an irreducible representation of $SO(3)$ with Casimir K), κ labels the quantum numbers K^{PC} of the gluonic degrees of freedom. For our case $\mathbf{G}^a = \mathbf{B}^a$ with $K^{PC} = 1^{+-}$. The spectrum of the mass eigenvalues, Λ_κ, called the gluelump mass, has been computed on the lattice in Refs. [22, 24, 49] and it is given by the gluelump correlator $\Lambda_\kappa = \lim_{T \to \infty} i/T \ln\langle\Omega|G_\kappa^a(T/2)\phi_{ab}(T/2, -T/2)G_\kappa^b(-T/2)|\Omega\rangle$.

The static energy E_Γ calculated in NRQCD at small r can be matched to the following objects in BOEFT:

$$E_\Gamma \equiv E_{\kappa,\lambda} = V_{\kappa,\lambda}^{(0)} = \frac{\alpha_s}{6r} + \Lambda_\kappa + a_{\kappa\lambda}r^2 + \cdots \tag{13}$$

where $\alpha_s/6r$ is the static octet potential, $a_{\kappa\lambda}$ is a nonperturbative coefficient that has a field theoretical definition and starts to depend on λ (instead that only on κ), which makes clear that at the NLO order in the multipole expansion the system is no longer spherically symmetric but acquires instead a cylindrical symmetry around the heavy-quark-antiquark axis. Therefore it is convenient to work with a basis of states with good transformation properties under $D_{\infty h}$. Such states can be constructed by projecting the gluelump operators on various directions with respect to the heavy-quark-antiquark axis. We define the degrees of freedom of the BOEFT as the operator $\hat{\Psi}_{\kappa\lambda}(\mathbf{r}, \mathbf{R}, t)$ defined by

$$P_{\kappa\lambda}^{i\dagger}O^a(\mathbf{r}, \mathbf{R}, t)\, G_\kappa^{ia}(\mathbf{R}, t) = Z_\kappa^{1/2}\hat{\Psi}_{\kappa\lambda}(\mathbf{r}, \mathbf{R}, t)\,, \tag{14}$$

the Z is a field renormalization, $P_{\kappa\lambda}^i$ is a projector that projects the gluelump operator to an eigenstate of $\mathbf{K} \cdot \hat{\mathbf{r}}$ with eigenvalue λ. For our case the projectors P_λ^i read $P_0^i = \hat{r}_0^i = \hat{r}^i$, $P_{\pm 1}^i = \hat{r}_\pm^i = \mp\left(\hat{\theta}^i \pm i\hat{\phi}^i\right)/\sqrt{2}$, with $\hat{\mathbf{r}} = (\sin(\theta)\cos(\phi), \sin(\theta)\sin(\phi), \cos(\theta))$, $\hat{\boldsymbol{\theta}} = (\cos(\theta)\cos(\phi), \cos(\theta)\sin(\phi), -\sin(\theta))$, $\hat{\boldsymbol{\phi}} = (-\sin(\phi), \cos(\phi), 0)$. The BOEFT is obtained by integrating out modes of scale Λ_{QCD}, i.e. the gluonic excitation and the Lagrangian reads as

$$L_{\text{BOEFT}} = \int d^3R d^3r \sum_\kappa \sum_{\lambda\lambda'} \text{Tr}\{\hat{\Psi}_{\kappa\lambda}^\dagger(\mathbf{r}, \mathbf{R}, t)[i\partial_t - V_{\kappa\lambda\lambda'}(r) + P_{\kappa\lambda}^{i\dagger}\frac{\nabla_r^2}{m}P_{\kappa\lambda'}^i]\hat{\Psi}_{\kappa\lambda'}(\mathbf{r}, \mathbf{R}, t)\} + \dots, \tag{15}$$

where the trace is over spin indices of the heavy quark and antiquark, and the ellipsis stands for operators producing transitions to standard quarkonium states and transitions between hybrid states of different κ. The latter are suppressed at least by $1/\Lambda_{\text{QCD}}$ since the static energies for different κ are separated by a gap $\sim \Lambda_{\text{QCD}}$. The interesting points of the Lagrangian above is that the kinetic operator is not commuting with the projector, which induces a non adiabatic coupling, already known from molecular physics.

The potential $V_{\kappa\lambda\lambda'}$ can be organized into an expansion in $1/m$ and a sum of static, spin-dependent (SD) and independent (SI) parts to be calculated in the matching with NRQCD. In Ref. [51] the static potential $V_{\kappa\lambda}^{(0)}(r)$ was matched to the quark-antiquark hybrid static energies computed on the lattice and the matrix elements of $P_{\kappa\lambda}^{i\dagger}\frac{\nabla_r^2}{m}P_{\kappa\lambda'}^i$ were obtained for $\kappa = 1^{+-}$ and shown to contain off-diagonal terms in λ-λ' that lead to coupled Schrödinger equations:

$$\left[-\frac{1}{Mr^2}\partial_r r^2 \partial_r + \frac{1}{Mr^2}\begin{pmatrix} l(l+1)+2 & 2\sqrt{l(l+1)} \\ 2\sqrt{l(l+1)} & l(l+1) \end{pmatrix} + \begin{pmatrix} E_{\Sigma_u^-} & 0 \\ 0 & E_{\Pi_u} \end{pmatrix}\right]\begin{pmatrix} \psi_\Sigma^{(N)} \\ \psi_{-\Pi}^{(N)} \end{pmatrix} = \mathcal{E}_N \begin{pmatrix} \psi_\Sigma^{(N)} \\ \psi_{-\Pi}^{(N)} \end{pmatrix}, \quad (16)$$

$$\left[-\frac{1}{Mr^2}\partial_r r^2 \partial_r + \frac{l(l+1)}{Mr^2} + E_{\Pi_u}\right]\psi_{+\Pi}^{(N)} = \mathcal{E}_N \psi_{+\Pi}^{(N)}, \quad (17)$$

where l is the total orbital angular momentum quantum number sum $\mathbf{L} = \mathbf{L}_{Q\bar{Q}} + \mathbf{K}$, $\mathcal{E}_N$ are the hybrids energies and $E_{\Sigma_u^-}$ and E_{Π_u} have been written in BOEFT in term of the static potentials plus the gluelump mass taken from [24]: $\Lambda_{1^{+-}} = 0.87(15)$ GeV[3].

The Schrödinger equations were solved numerically and the spectrum and wave functions of hybrid states generated the static energies labeled by Σ_u^- and Π_u were obtained, precisely:

The functions $\psi_\Sigma^{(N)}$ and $\psi_{\pm\Pi}^{(N)}$ are radial wave functions; $\psi_\Sigma^{(N)}$ and $\psi_{-\Pi}^{(N)}$ have negative parity and $\psi_{+\Pi}^{(N)}$ positive one. The off-diagonal terms change the Σ wave function to Π and vice versa, but they do not change the parity. Hence $\psi_\Sigma^{(N)}$ mixes only with $\psi_{-\Pi}^{(N)}$, and $\psi_{+\Pi}^{(N)}$ decouples. For $l = 0$ the off-diagonal terms vanish, so the equations for $\psi_\Sigma^{(N)}$ and $\psi_{-\Pi}^{(N)}$ decouple; there exists only one parity state, and its radial wave function is given by a Schrödinger equation with the E_Σ potential and an angular part $2/Mr^2$. The eigenstates of the equations (16) and (17) are organized in the multiplets shown in Table 1 (all the J^{PC} quantum numbers of a given multiplet will be degenerate up to when we will consider spin dependent interactions in Sec. 3.1.2).

	l	$J^{PC}\{s = 0, s = 1\}$	E_Γ
H_1	1	$\{1^{--}, (0, 1, 2)^{-+}\}$	$E_{\Sigma_u^-}, E_{\Pi_u}$
H_2	1	$\{1^{++}, (0, 1, 2)^{+-}\}$	E_{Π_u}
H_3	0	$\{0^{++}, 1^{+-}\}$	$E_{\Sigma_u^-}$
H_4	2	$\{2^{++}, (1, 2, 3)^{+-}\}$	$E_{\Sigma_u^-}, E_{\Pi_u}$
H_5	2	$\{2^{--}, (1, 2, 3)^{-+}\}$	E_{Π_u}

Table 1: J^{PC} multiplets with $l \leq 2$ for the Σ_u^- and Π_u gluonic states. The last column shows the gluonic static energies that appear in the Schrödinger equation of the respective multiplet.
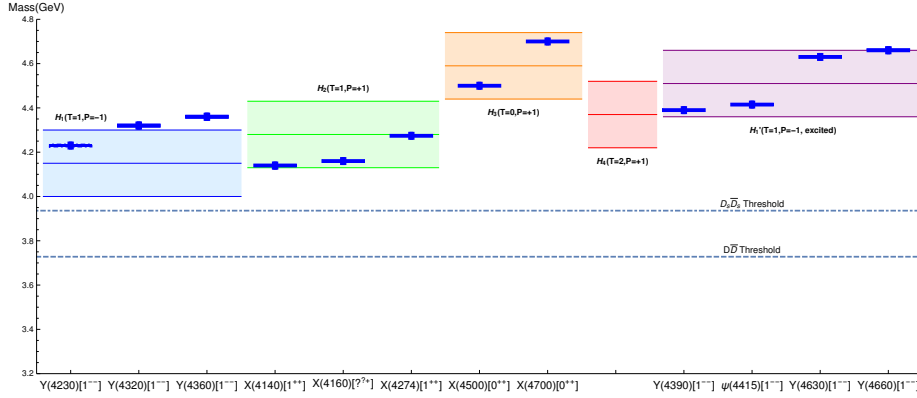
3.1.1 Spectrum

Keeping in the equations (16) and (17) only the heavy quark-antiquark kinetic energy and the hybrid static energies, E_Γ, amounts at the *Born–Oppenheimer approximation*. Keeping only the diagonal terms amounts at the *adiabatic approximation*. The exact leading order equations include both diagonal and off-diagonal terms that define the so-called *non-adiabatic coupling*. As it is clear from (16) and (17) both diagonal and off-diagonal terms contribute at the same order to the energy levels in the quarkonium hybrid case. This situation is different from the case of (electromagnetic)

---

[3]Note that the gluelump mass is a scheme dependent quantity like the quark mass, here it is calculated in RS scheme.
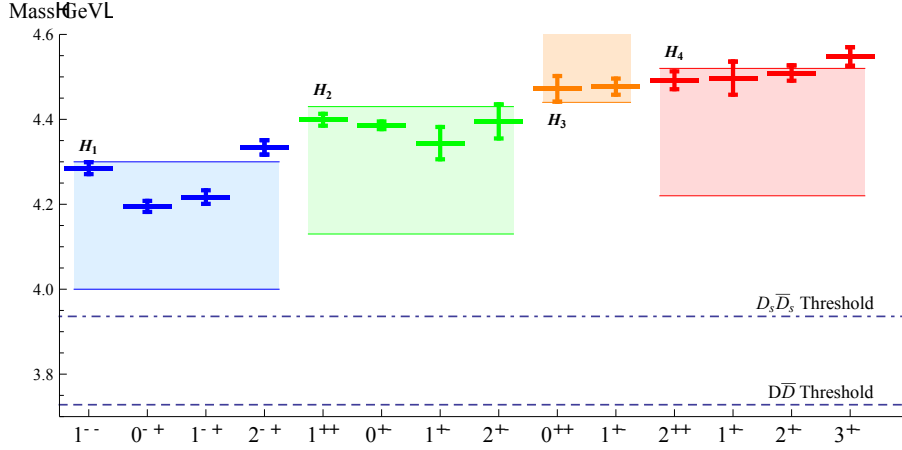
Figure 5: Comparison of results from the direct lattice computations of charmonium hybrid masses of [50] with the results of [51]. The direct lattice mass predictions are plotted in solid lines with error bars corresponding to the mass uncertainties. Our results for the H1, H2, H3, and H4 multiplets have been plotted in error bands corresponding to the gluelump mass uncertainty of ±0.15 GeV.

molecules, where the non-adiabatic coupling is subleading [52]. A physical consequence of the mixing is the so-called Λ *doubling*, i.e., the lifting of degeneracy between states with the same parity. We show this effect in Fig. 5, where you see that the multiplets H_1 and H_2 are not degenerate and this effect is also confirmed in direct lattice evaluations. The same effect would be seen also between H_4 and H_5 [51]. The effect is also present in molecular physics, however, Λ doubling is a subleading effect there.

Figure 6: Mass spectrum of neutral exotic charmonium states obtained by solving Eqs. (16) and (17). The experimental states of Sec. 3.1 that have matching quantum numbers are plotted in solid blue lines. In the figure T stay for the total angular momentum. H_1' is the first H_1 radial excitation of H_1. The multiplets have been plotted with error bands corresponding to a gluelump mass uncertainty of 0.15 GeV. Figure taken from [1].

Several charmonium-like states have been found by the B factories in the last decade (for a recent review see [1]). We compare some of these states with the hybrid spectrum obtained from solving the coupled Schrödinger equations (16) and (17) in Fig. 6. In the bottomonium sector, the

state $Y_b(10890)[1^{--}]$ with mass $M_{Y_b} = (10.8884 \pm 3.0)$ GeV found by BELLE may be a possible H_1 candidate, for which we find $M_{H_1} = (10.79 \pm 0.15)$ GeV. *This picture allows us to describe the spectrum of hybrids within an EFT description of QCD (which should be equivalent to QCD in the taken window) plus lattice input. It is complementary to direct lattice evaluations of the spectrum in many ways: first of all it is simpler and allows to get all the flavour of hybrids on the basis of the evaluation of few correlators only dependent on the gluonic degrees of freedom, it takes advantage of factorization and it lends an interpretation to the underlying physics. The multiplets that we have obtained are distinctive of the underlying physics: if one would construct the hybrids multiplets using the constituent gluon picture for example a different multiplet structure would be obtained [51]. Of course in order to validate the experimental identifications one has to add the spin structure, and especially consider decays and production features: also this may turn out to be simpler in the BOEFT approach.*
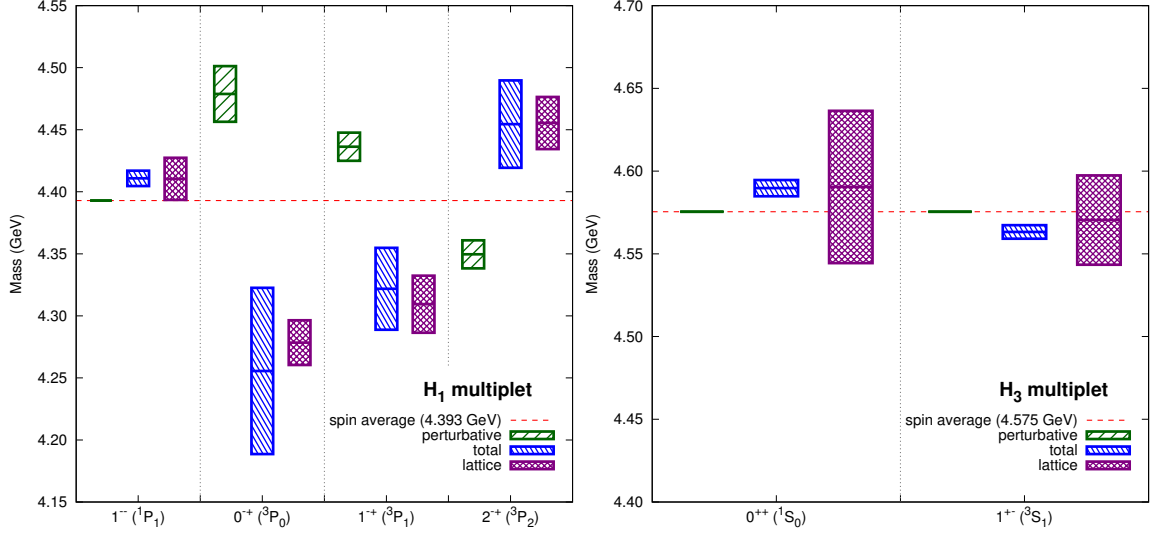
3.1.2 Spin effects in Hybrids

The spin of the quarks has been considered in direct lattice calculations of the hybrids mass, mostly in charmonium for quenched and noncontinuum extrapolated data [55], recently in unquenched and continuum extrapolated data [57] and recently in bottomonium [56]. It is rare to see spin effects treated in models and, in case they are considered, it is on the basis of a gluon constitutent picture or extrapolating from the standard quarkonium spin structure, which we will see is not the appropriate thing to do. In BOEFT we could obtain for the first time the spin dependent potentials (for $\kappa = 1^{+-}$, λ takes the values $0, \pm1$) [53, 54, 58]:

$$
\begin{aligned}
V^{(1)}_{\lambda\lambda' SD}(r) =\ & V_{SK}(r)\left(P^{i\dagger}_\lambda K^{ij} P^j_{\lambda'}\right) \cdot \boldsymbol{S} \\
& + V_{SKb}(r)\left[\left(\boldsymbol{r}\cdot\boldsymbol{P}^\dagger_\lambda\right)\left(r^i K^{ij} P^j_{\lambda'}\right)\cdot\boldsymbol{S} - \left(r^i K^{ij} P^{j\dagger}_\lambda\right)\cdot\boldsymbol{S}\left(\boldsymbol{r}\cdot\boldsymbol{P}_{\lambda'}\right)\right],
\end{aligned} \tag{18}
$$

$$
\begin{aligned}
V^{(2)}_{\lambda\lambda' SD}(r) =\ & V_{SLa}(r)\left(P^{i\dagger}_\lambda \boldsymbol{L}_{Q\bar{Q}} P^i_{\lambda'}\right)\cdot\boldsymbol{S} + V_{SLb}(r)P^{i\dagger}_\lambda\left(L^i_{Q\bar{Q}} S^j + S^i L^j_{Q\bar{Q}}\right)P^j_{\lambda'} \\
& + V_{SLc}(r)\left[\left(\boldsymbol{r}\cdot\boldsymbol{P}^\dagger_\lambda\right)(\boldsymbol{p}\times\boldsymbol{S})\cdot\boldsymbol{P}_{\lambda'} + \boldsymbol{P}^\dagger_\lambda\cdot(\boldsymbol{p}\times\boldsymbol{S})(\boldsymbol{r}\cdot\boldsymbol{P}_{\lambda'})\right] \\
& + V_{S^2}(r)\boldsymbol{S}^2\delta_{\lambda\lambda'} + V_{S_{12}a}(r)S_{12}\delta_{\lambda\lambda'} + V_{S_{12}b}(r)P^{i\dagger}_\lambda P^j_{\lambda'}\left(S^i_1 S^j_2 + S^i_2 S^j_1\right),
\end{aligned} \tag{19}
$$

where $\left(K^{ij}\right)^k = i\epsilon^{ikj}$ is the angular momentum operator for the spin-1 gluonic excitation and $\boldsymbol{L}_{Q\bar{Q}}$ is the orbital angular momentum of the heavy-quark-antiquark pair, $\boldsymbol{S}$ is the total spin of the quarks, and the projectors for $\kappa = 1^{+-}$ have been previously defined. The $1/m$ operators in Eq. (18), with coefficients $V_{SK}(r)$ and $V_{SKb}(r)$ couple the angular momentum of the gluonic excitation with the total spin of the heavy-quark-antiquark pair. These operators are characteristic of the hybrid states and are absent for standard quarkonia. Among the $1/m^2$ operators in Eq. (19), the operators with coefficients $V_{SLa}(r)$, $V_{S^2}(r)$, and $V_{S_{12}a}$ are the standard spin-orbit, total spin squared, and tensor spin operators respectively, which appear for standard quarkonia also. In addition to them, three novel operators appear at order $1/m^2$. The operators with coefficients $V_{SLb}(r)$ and $V_{SLc}(r)$ are generalizations of the spin-orbit operator to the hybrid states. Similarly, the operator with coefficient $V_{S_{12}b}(r)$ is generalization of the tensor spin operator to the hybrid states. *Quite interestingly, differently from the quarkonium case, the hybrid potential gets a first contribution already at order Λ^2_{QCD}/m. The corresponding operator does not contribute at LO*
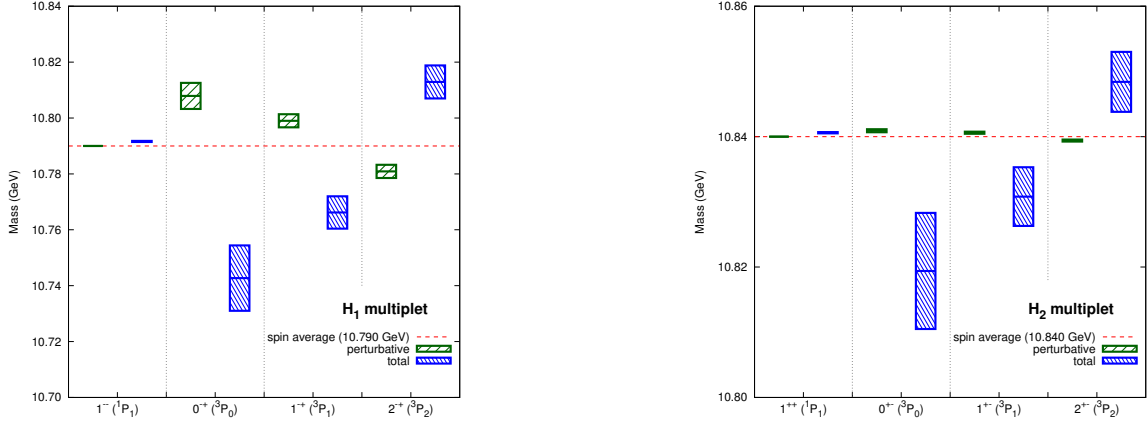
Figure 7: Spectrum of H_1 and $H3$ charmonium hybrid multiplets (including the spin effects). The lattice results from [55] [2+1 flavors, $m_\pi = 240$ MeV] are plotted in purple. In green we plotted the perturbative contributions to the spin-dependent operators in Eq. (19) added to the spin average of the lattice results (red dashed line). In blue we show the full result of the spin-dependent operators of Eqs. (18)-(19) including both the perturbative and nonperturbative contributions. The unknown nonperturbative matching coefficients are determined by comparing the charmonium hybrid spectrum obtained from the BOEFT to the lattice data. The height of the boxes indicate the uncertainty as detailed in [53], there you find the spectrum for all the multiplets.

to matrix elements of quarkonium states as its projection on quark-antiquark color singlet states vanishes. Hence, spin splittings are remarkably less suppressed in heavy quarkonium hybrids than in heavy quarkonia: this will have a notable impact on the phenomenology of exotics.

The coefficients $V_i(r)$ on the right-hand side of Eqs. (18) and (19) have the form $V_i(r) = V_{oi}(r) + V_i^{np}(r)$, where $V_{oi}(r)$ is the perturbative octet potential and $V_i^{np}(r)$ is the nonperturbative contribution in the case in which $1/r \ll \Lambda_{QCD}$. The octet part can be calculated in perturbation theory while the nonperturbative part is given in terms of purely gluonic correlators whose detailed form is given in [53] (or they are given in term of generalized Wilson loops with hybrids as initial and final states in the case in which $1/r \sim \Lambda_{QCD}$). There are eight of these nonperturbative correlators that have not yet been calculated on the lattice, therefore we fix them on direct lattice determination of the charmonium hybrid masses. In [53] we used data from the Hadron Spectrum Collaboration one set from Ref. [50] with a pion mass of $m_\pi \approx 400$ MeV and a more recent set from Ref. [55] with a pion mass of $m_\pi \approx 240$ MeV. For all the details of the fit we refer to [53] . We take the values $m_c^{RS}(1\text{GeV}) = 1.477$ GeV and α_s at 4-loops with three light flavors, $\alpha_s(2.6 \text{ GeV}) = 0.26$.

An interesting feature is that for the spin-triplets, the value of the perturbative contributions decreases with J. This trend is opposite to that of the lattice results. This discrepancy can be reconciled thanks to the nonperturbative contributions, in particular due to the contribution from $V_{SK}^{np\,(0)}$, which is only suppressed by $1/m$, and has no perturbative counterpart. A consequence of this is that a model calculation with a spin interaction inspired by quarkonium physics would give the wrong result.

Figure 8: Spectrum of H_2 and H_1 bottomonium hybrids multiplets, nonperturbative correlators fixed on charmonium hybrids. In green we plotted the perturbative contributions to the spin-dependent operators in Eq. (19) added to the spin average of the lattice results (red dashed line). In blue we show the full result of the spin-dependent operators of Eqs. (18)-(19) including both the perturbative and nonperturbative contributions. The height of the boxes indicate the uncertainty as detailed in [53], there you find the spectrum for all the multiplets.

All the dependence on the heavy-quark mass of the $V^{np\,(i)}$ is encoded in the NRQCD matching coefficients c_F and c_s. At leading order in α_s these coefficients are known to be equal to 1 and the dependence on the heavy-quark mass only appears when the next-to-leading order is considered. At the order we are working, only the heavy-quark mass dependence of c_F is relevant, we use its one-loop expression, with the renormalization scale set as the heavy-quark mass. Taking this mass dependence into account, we can use the set of nonperturbative parameters (that are flavor independent) to predict the spin contributions in the bottomonium hybrid sector, for which lattice determinations are difficult to obtain. We present the results for two multiplets in Fig. 8, you can find the other multiplets in [53].

This is a nice example of the huge predictivity that BOEFT plus lattice input can achieve: once the nonperturbative correlators are fixed on lattice data for charmonium hybrids (or better when these low energy correlators will be directly calculated on the lattice) then we can predict all the bottomonia (and B_c) hybrids multiplets.

3.1.3 Tetraquarks, Decays, Production

BOEFT may be used to describe also tetraquarks. In this case, it is necessary to compute on the lattice generalized Wilson loops of the type given in Eq. (11) where the operator P_Γ^a contains also appropriate light quark operators and besides the Λ_η^σ and κ also the isospin quantum numbers $I = 0, 1$ have to be considered. The same approach can be used also to describe pentaquarks [52, 58]. The light quark plays a similar role to the gluonic excitations in the hybrid case. These static energies, for which few pioneering lattice studies exist [61–63], are a crucial ingredient to provide for the first time a dynamical description of tetraquarks in QCD. When these objects will be made available, it will be interesting to study the behaviour of the static energies near the avoided level crossing with the heavy-light meson-meson thresholds [66]. Decays of hybrids and tetraquarks as well as and mixing of hybrids and tetraquarks with other quarkonium states could be studied and

computed in BOEFT, however lattice input on few correlators purely depending on the glue would be needed [59].

3.2 Tetraquarks, molecules, hadroquarkonium ?

In this BOEFT/Lattice picture we will have all of the above descriptions contributing [60]. When looking at the actual plot of a static energy as a function of r for a state with $Q\bar{Q}q\bar{q}$ or $Q\bar{Q}g$ we will have different regions: for short distance a hadroquarkonium picture would emerge, then a tetraquark (or hybrid) one and when passing the the heavy-light mesons line, threshold effects should have to be taken into account and a molecular picture would emerge. However QCD would dictate, throught the lattice correlators and the BOEFT characteristics and power counting, which structure would dominate and in which precise way.

3.3 Input needed from the lattice

Summarizing, to address the X Y Z states we need input from the lattice:

- Besides the hybrids static energies we need all the tetraquark static energies in the short and long distance, extrapolated to continuum, calculated with the generalized Wilson loop mentioned in 3.2. Some pioneering calculations exist [61–63] but more should be done.

- We need lattice calculations of the nonperturbative correlators entering the spin dependent hybrids and tetraquark potentials: they are gauge invariant correlators of chromolectric and chromomagnetic fields and gluelump operators (without the color octet quark part).

- We need lattice calculations of three point functions containing the information of the quarkonium/hybrids quarkonium/tetraquarks mixing.

- Lattice results about the crosstalk of the static energies with a pair of heavy-light mesons in the lattice appeared [64–66] but further investigations appear to be necessary.

This will be instrumental to tackle the X Y Z states in QCD.

4. Outlook

We have shown that there is a vital interplay between EFTs and lattice for what concerns Exotics. NREFTs are vital to define objects of great phenomenological interest and give a systematic scheme to calculate physical observables, as well as an understanding of the underlying degrees of freedom and dynamics.

NREFTs are based on factorization which allows to encode all the nonperturbative effects in low energy correlators, depending only on chromoelectric and chromomagnetic fields. This enhances the predictivity of the theory since the same correlators can be used in the charmonium and bottomonium sectors eliminating for example the difficulties of direct lattice calculations of exotics at the high mass of the bottom. Moreover, once the lattice has provided the nonperturbative input on the correlators, the calculation of the physical properties ranging from masses, decays, transitions and production, follow inside the BOEFT, which is much simpler and under control

that repeating a lattice calculation for each of these observables. Of course there are challenges: the calculation of correlator of chromoelectric and chromomagnetic fields display bad convergence properties on the lattice see e.g. [46] and references therein. The gradient flow method seems however to help tremendously here, e.g. see [47, 67] There may be still difficulties related to change of renormalization schemes between the continuum of the BOEFT and the lattice regularization. For physical objects like the force there are no issues and a gradient flow calculation in continuum can help the lattice extrapolations [48].

We regard the combination of BOEFTs and Lattice QCD as very promising to attack the physics of the X, Y, Z on the basis of QCD. We have seen that Lattice is crucial to gain predictivity in these NREFTs calculations, on the other hand the NREFTs allow to use lattice results in an array of problems that often are not in its reach like nonequilibrium evolution, production processes and in general to develop a convenient and complementary avenue to address exotics.

References

[1] N. Brambilla, S. Eidelman, C. Hanhart, A. Nefediev, C. P. Shen, C. E. Thomas, A. Vairo and C. Z. Yuan, Phys. Rept. **873** (2020), 1-154.

[2] N. Brambilla, S. Eidelman, B. K. Heltsley, R. Vogt, G. T. Bodwin, E. Eichten, A. D. Frawley, A. B. Meyer, R. E. Mitchell and V. Papadimitriou, *et al.* Eur. Phys. J. C **71** (2011), 1534.

[3] N. Brambilla *et al.* [Quarkonium Working Group], [arXiv:hep-ph/0412158 [hep-ph]].

[4] N. Brambilla, S. Eidelman, P. Foka, S. Gardner, A. S. Kronfeld, M. G. Alford, R. Alkofer, M. Butenschoen, T. D. Cohen and J. Erdmenger, *et al.* Eur. Phys. J. C **74** (2014) no.10, 2981.

[5] M. Tanabashi *et al.* [Particle Data Group], Phys. Rev. D **98** (2018) no.3, 030001.

[6] S. K. Choi *et al.* [Belle], Phys. Rev. Lett. **91** (2003), 262001.

[7] A. Ali, J. S. Lange and S. Stone, Prog. Part. Nucl. Phys. **97** (2017), 123-198.

[8] F. K. Guo, C. Hanhart, U. G. Meißner, Q. Wang, Q. Zhao and B. S. Zou, Rev. Mod. Phys. **90** (2018) no.1, 015004.

[9] E. Braaten and M. Lu, Phys. Rev. D **76** (2007), 094028.

[10] E. Braaten and M. Kusunoki, Phys. Rev. D **69** (2004), 074005.

[11] S. Fleming and T. Mehen, Phys. Rev. D **85** (2012), 014016.

[12] E. Braaten, C. Langmack and D. H. Smith, Phys. Rev. D **90** (2014) no.1, 014044.

[13] E. Braaten, C. Langmack and D. H. Smith, Phys. Rev. Lett. **112** (2014), 222001.

[14] https://einrichtungen.ph.tum.de/T30f/tumqcd/index.html

[15] A. V. Manohar, Phys. Rev. D **56** (1997), 230-237.

[16] N. Brambilla, D. Gromes and A. Vairo, Phys. Lett. B **576** (2003), 314-327.

[17] W. E. Caswell and G. P. Lepage, Phys. Lett. B **167** (1986), 437-442.

[18] G. T. Bodwin, E. Braaten and G. P. Lepage, Phys. Rev. D **51** (1995), 1125-1171.

[19] N. Brambilla, A. Pineda, J. Soto and A. Vairo, Rev. Mod. Phys. **77** (2005), 1423.

[20] A. Pineda and J. Soto, Nucl. Phys. B Proc. Suppl. **64** (1998), 428-432.

[21] N. Brambilla, A. Pineda, J. Soto and A. Vairo, Nucl. Phys. B **566** (2000), 275.

[22] M. Foster *et al.* [UKQCD], Phys. Rev. D **59** (1999), 094509.

[23] K. J. Juge, J. Kuti and C. Morningstar, Phys. Rev. Lett. **90** (2003), 161601.

[24] G. S. Bali and A. Pineda, Phys. Rev. D **69** (2004), 094001.

[25] L. Müller, O. Philipsen, C. Reisinger and M. Wagner, Phys. Rev. D **100** (2019) no.5, 054503.

[26] C. Schlosser and M. Wagner, [arXiv:2111.00741 [hep-lat]].

[27] N. Brambilla, A. Pineda, J. Soto and A. Vairo, Phys. Rev. D **63** (2001), 014023.

[28] A. Pineda and A. Vairo, Phys. Rev. D **63** (2001), 054007.

[29] N. Brambilla, V. Leino, P. Petreczky and A. Vairo, Phys. Rev. D **102** (2020) no.7, 074503.

[30] G. S. Bali, K. Schilling and A. Wachter, Phys. Rev. D **56** (1997), 2566-2589.

[31] G. S. Bali, Phys. Rept. **343** (2001), 1-136.

[32] Y. Koma, M. Koma and H. Wittig, Phys. Rev. Lett. **97** (2006), 122003.

[33] Y. Koma and M. Koma, PoS **LATTICE2012** (2012), 140.

[34] Y. Koma and M. Koma, AIP Conf. Proc. **1322** (2010) no.1, 298-306.

[35] N. Brambilla, D. Eiras, A. Pineda, J. Soto and A. Vairo, Phys. Rev. D **67** (2003), 034018. [36]

[36] N. Brambilla, H. S. Chung and A. Vairo, Phys. Rev. Lett. **126** (2021) no.8, 082003.

[37] N. Brambilla, H. S. Chung and A. Vairo, JHEP **09** (2021), 032.

[38] N. Brambilla, PoS **HardProbes2020** (2021), 017.

[39] D. Bala, O. Kaczmarek, R. Larsen, S. Mukherjee, G. Parkar, P. Petreczky, A. Rothkopf and J. H. Weber, [arXiv:2110.11659 [hep-lat]].

[40] N. Brambilla, M. A. Escobedo, A. Vairo and P. Vander Griend, Phys. Rev. D **100** (2019) no.5, 054025.

[41] N. Brambilla, M. A. Escobedo, J. Soto and A. Vairo, Phys. Rev. D **97** (2018) no.7, 074009.

[42] N. Brambilla, M. Á. Escobedo, M. Strickland, A. Vairo, P. Vander Griend and J. H. Weber, JHEP **05** (2021), 136.

[43] L. Altenkort, A. M. Eller, O. Kaczmarek, L. Mazur, G. D. Moore and H. T. Shu, Phys. Rev. D **103** (2021) no.1, 014511.

[44] G. Aarts, C. Allton, S. Kim, M. P. Lombardo, M. B. Oktay, S. M. Ryan, D. K. Sinclair and J. I. Skullerud, JHEP **11** (2011), 103.

[45] S. Kim, P. Petreczky and A. Rothkopf, JHEP **11** (2018), 088.

[46] N. Brambilla, V. Leino, O. Philipsen, C. Reisinger, A. Vairo and M. Wagner, [arXiv:2106.01794 [hep-lat]].

[47] V. Leino, N. Brambilla, O. Philipsen, C. Reisinger, A. Vairo and M. Wagner, [arXiv:2111.07916 [hep-lat]].

[48] N. Brambilla, H. S. Chung, A. Vairo and X. P. Wang, [arXiv:2111.07811 [hep-ph]].

[49] K. Marsh and R. Lewis, Phys. Rev. D **89** (2014) no.1, 014502 [arXiv:1309.1627 [hep-lat]].

[50] L. Liu *et al.* [Hadron Spectrum], JHEP **07** (2012), 126 [arXiv:1204.5425 [hep-ph]].

[51] M. Berwein, N. Brambilla, J. Tarrús Castellà and A. Vairo, Phys. Rev. D **92** (2015) no.11, 114019.

[52] N. Brambilla, G. Krein, J. Tarrús Castellà and A. Vairo, Phys. Rev. D **97** (2018) no.1, 016016.

[53] N. Brambilla, W. K. Lai, J. Segovia and J. Tarrús Castellà, Phys. Rev. D **101** (2020) no.5, 054040.

[54] N. Brambilla, W. K. Lai, J. Segovia, J. Tarrús Castellà and A. Vairo, Phys. Rev. D **99** (2019) no.1, 014017.

[55] G. K. C. Cheung *et al.* [Hadron Spectrum], JHEP **12** (2016), 089.

[56] S. M. Ryan *et al.* [Hadron Spectrum], JHEP **02** (2021), 214 [arXiv:2008.02656 [hep-lat]].

[57] G. Ray and C. McNeile, [arXiv:2110.14101 [hep-lat]].

[58] J. Soto and J. Tarrús Castellà, Phys. Rev. D **102** (2020) no.1, 014012.

[59] R. Oncala and J. Soto, Phys. Rev. D **96** (2017) no.1, 014004.

[60] J. Tarrús Castellà, EPJ Web Conf. **202** (2019), 01005.

[61] M. Sadl and S. Prelovsek, [arXiv:2109.08560 [hep-lat]].

[62] S. Prelovsek, H. Bahtiyar and J. Petkovic, Phys. Lett. B **805** (2020), 135467

[63] P. Bicudo, K. Cichy, A. Peters and M. Wagner, Phys. Rev. D **93** (2016) no.3, 034501

[64] G. S. Bali *et al.* [SESAM], Phys. Rev. D **71** (2005), 114513

[65] J. Bulava, B. Hörz, F. Knechtli, V. Koch, G. Moir, C. Morningstar and M. Peardon, Phys. Lett. B **793** (2019), 493-498

[66] R. Bruschini and P. González, [arXiv:2111.07653 [hep-ph]].

[67] V. Leino, N. Brambilla, J. Mayer-Steudte, A. Vairo "The static force from generalized Wilson loops using gradient flow", TUM-EFT 157/21